

# A $sp^3$ -type mono-vacancy defect in graphene based Möbius strip

Xianlong Wang, Xiaohong Zheng and Zhi Zeng\*

*Key Laboratory of Materials Physics, Institute of Solid State Physics,*

*Chinese Academy of Sciences, Hefei 230031, P.R. China*

(Dated: January 10, 2013)

## Abstract

By using first-principles method combined with molecular dynamics simulations, the structural and electronic properties of mono-vacancy (MV) defect in Möbius strip formed from graphene are investigated. Two kinds of MV are observed depending on the local structures around defects. In the curved areas of Möbius strip, MV has the configuration of one pentagon and one nonagon ring (59-type), which is similar to that of carbon nanotube and graphene. Interestingly, the most stable MV appear in the twisted areas and acquires novel structure, which has two pentagon and two hexagon rings (5566-type) and one  $sp^3$  hybridized carbon at the central site. Molecular dynamics simulations furthermore prove that in Möbius strip, both normal 59-type and novel 5566-type MV is a stable configuration at room temperature. Furthermore, it is expected that 5566-type MV is a popular MV pattern and will give rise to  $sp^3$ -type bonding in carbon based low-dimension materials with chiral twisting.

---

\* Correspondence author: zzeng@theory.issp.ac.cn

## I. INTRODUCTION

Recently, one novel carbon nanostructure, graphene based Möbius strip (GMS), has attracted extensive attention due to its special topological property, namely, with only one face and one edge. It is totally different from that of other carbon based low-dimension materials, such as carbon nanotube and graphene. Carbon based Möbius strips were already synthesized in experiments[1, 2] and widely investigated by theoretical researchers.[3–11] Their results demonstrate that GMS is a stable structure,[9] and show novel optical [4, 10] and magnetic properties.[6, 10] Especially, it may even behave as a topological insulator.[7]

Since carbon based materials are usually not ideal crystals and atomic vacancies can affect their properties significantly,[12–14] such as inducing magnetism in graphene,[14] great attention has been focused on the study of atomic vacancies presented in carbon nanotube and graphene,[13–20] where atomic vacancies can be introduced unintentionally during the processes of synthesis or deliberately by irradiation, chemical and plasma treatments. Among different types of atomic vacancies in carbon nanostructures, mono-vacancy (MV) with one atom missing from lattice is a simple, popular and attractive one and has been identified clearly by experimentalists and theorists in carbon nanotube and graphene.[19–23] In these systems, MV undergoes a Jahn-Teller distortion, which leads to the formation of covalent bond between two of three atoms located around the atomic vacancy and results in one five-membered ring and one nine-membered ring (59-type MV). To date, only 59-type MV was reported in both carbon nanotube and graphene.

Just like carbon nanotube and graphene, to fully understand the properties of GMS for its potential applications, it is important and necessary to illustrate its MV properties. First of all, the structural configurations of the MV present in GMS should be clarified. As shown in our previous work,[9] since each GMS is composed by two kinds of areas, curved and chiral twisted parts, the MV features of GMS should be investigated separately depending on its local structures. In this work, by taking use of first-principles method we illustrate the structural and electronic properties of the MV in GMS. Interestingly, besides 59-type MV present in the curved area, a novel 5566-type MV, which has two pentagon and two hexagon and acquires one  $sp^3$  carbon atom at the central site, is observed in the twisted region. To the best of our knowledge, the 5566-type MV has never been reported in carbon based low-dimension materials before. Furthermore, due to the strain introduced by their edges,

graphene nanoribbons (GNR) with chiral twist were theoretically predicted,[24–27] and in fact experimentally observed.[29] Especially, in a very recent experiment,[30] the shapes of GNR with different chiral twisted degrees were clearly shown by transmission electron microscopy (TEM) images. Since graphene nanoribbons can indeed be transformed into carbon nanotubes through chiral twisting,[31] and the local configurations of the twisted areas of GMS are similar to that of GNR with chiral twisting, we predict that 5566-type MV is also observable in chirally twisted carbon nanotubes and graphene.

## II. COMPUTATIONAL DETAILS

The calculations are performed by the widely adopted SIESTA package, in which a norm-conserving pseudopotential and linear combinations of atomic orbital basis sets are used.[32, 33] The wave function is expanded with a double- $\zeta$  (DZ) basis sets, and the exchange-correlation potential of generalized gradient approximation (GGA) with the form of Perdew-Burke-Ernzerhof (PBE) is selected.[34] The lattice vectors ( $50 \times 50 \times 50$  Å) are large enough to avoid the interactions from adjacent neighbors. All related structures are fully relaxed. The method and parameters used in this work are basically the same as that in our previous work.[9, 35] The accuracy of our procedure is tested by calculating the properties of MV in infinite graphene by taking use of  $12 \times 12$  supercell. Our results are in a good agreement with previous ones.[23]

## III. RESULTS AND DISCUSSIONS

In our previous work,[9] the structural features and formation energies of GMS as the function of their width-to-length ratio are characterized. We find that one, two and three planar triangle regions can be observed in GMS and their formation energies increase with the ratio of width-to-length increasing. Typically, a GMS model with the length of 30 armchair lines and the width of 6 zigzag lines is used to simulate the MV properties of GMS and such a structure has one planar triangle area. Due to its special topological structure, GMS can be separated to three different areas depending on local deformation. As shown in Fig. 1(a), A and C denote the areas with twisting, while B is the curved area similar to carbon nanotube. One carbon atom which is close to the center of A, B or C area is removed

from the GMS to create a MV and these MVs are hereafter denoted as MV-A, MV-B and MV-C, respectively. The formation energy ( $\Omega$ ) of MV in GMS (labeled as  $\Omega_{MV}$  (GMS)) and that in graphene (labeled as  $\Omega_{MV}(G)$ ) are respectively given by the following equations:

$$\Omega_{MV}(GMS) = E(GMS) - E_{MV}(GMS) - E_{\text{atom}}, \quad (1)$$

$$\Omega_{MV}(G) = E(G) - E_{MV}(G) - E_{\text{atom}}, \quad (2)$$

$$E_{\text{atom}} = E(G)/N. \quad (3)$$

where  $E(GMS)$  ( $E(G)$ ) and  $E_{MV}$  (GMS) ( $E_{MV}(G)$ ) denote the total energies of GMS(graphene) without and with MV, respectively, and  $N$  is the number of carbon atoms in a  $12 \times 12$  graphene supercell. The calculated results are presented in Table I, the formation energy of MV in graphene is 7.56 eV, which agrees well with that of the published results(7.4 eV[22] and 7.7 eV[23]). The formation energies of MV-A, MV-B and MV-C are respectively 6.43 eV, 6.51 eV and 6.72 eV, and all of them are about 1 eV smaller than that of graphene (7.56 eV), indicating that compared with infinite graphene, it will be much easier to introduce MVs in GMS or graphene with chiral twisting due to the strain existing in these twisted structures. Furthermore, the most stable site for MV in GMS is located at its planar triangle area (A area) since the formation energy of MV-A is the smallest one, as shown in Table I.

The relaxed MV structures are presented in Fig. 1(b-d), and the zoomed in views are shown in the corresponding insets to clearly illustrate their structures. Similar to the MV of carbon nanotube and graphene,[21–23] as can be found in Fig. 1(c), MV-B shows a typical 59-type pattern, with one pentagon and one enneagon, and a new bond is formed between atom 1 and atom 2 with the bond-length of 1.59 Å, which is much shorter by 0.98 Å than the distance (2.57 Å) between atom 0 and atom 1, due to the Jahn-Teller distortion. Interestingly, MV-A and MV-C created in the twisted areas finally evolve into a novel 5566-type pattern where the central carbon atom becomes  $sp^3$  hybridized after full relaxation. The structural properties of MV-A and MV-C are shown in Table II, and the results show that the averaged distance between the central carbon and its four neighbors is about 1.64 Å, which is significantly longer than the C-C bond-length (1.42 Å) in infinite graphene and slightly longer than that of the new bond formed in MV-B (1.59 Å) and the C-C bond in diamond (1.55 Å). Combined with the bond-angle information of MV-A and MV-C shown

also in Table II, we can conclude that the carbon atoms located at their central sites are of a  $sp^3$  type. To further confirm this, the electronic structures are studied, and Fig. 2(a) and (b) respectively present the partial density of states (PDOS) of edge carbon atoms of ideal GMS and the carbon atoms at the central sites of ideal planar triangle area. Meanwhile, the PDOS of the central carbon atom of MV-A is presented in Fig. 2(c). The carbon atom at the edge sites of GMS is spin polarized, which is similar to the case of graphene nanoribbons with zigzag edge and agrees with previous work.[9, 35] Furthermore, if we compare Fig. 2(b) with (c), the energy gap around the Fermi level shown in Fig. 2(c) is much larger than that of Fig. 2(b), the PDOS of a  $sp^2$  hybridized carbon, indicating that the central carbon atom of MV-A and MV-C is hybridized with its four neighbors by  $sp^3$ -like bonding.

Now we investigate whether this 5566-type MV is stable or not at room temperature. For this purpose, molecular dynamics simulations of MV-A and MV-B at room temperature ( $T = 300$  K) are carried out in the time step of 1 fs. The corresponding results of MV-A and MV-B are shown in Fig. 3 (a) and (b), respectively. After running 2000 steps, the MV geometry of 5566-type (MV-A) and 59-type (MV-B) pattern is still kept unchanged, suggesting that in Möbius strip formed from graphene, not only 59-type MV but also 5566-type MV containing a  $sp^3$  carbon atom is a stable configuration at room temperature. Finally, please note that, since the 5566-type MV can be formed at the areas with different degree of chiral twisting in the strip, such as A and C areas shown in Fig. 1(a), it should also be a popular MV configuration in carbon nanotube and graphene with chiral twists, which were actually observed in experiments.[29, 30] Furthermore, we expect that the  $sp^3$ -type features in this 5566-type MV can be probed by experiment, such as, X-ray photoelectron spectroscopy, in the chirally twisted carbon nanotube and graphene.

#### IV. CONCLUSION

The structural and electronic properties of mono-vacancy in Möbius strip formed from graphene are simulated. A novel mono-vacancy with 5566-type pattern with a  $sp^3$  hybridized carbon atom at its central site is observed in the chiral twisted areas, while a normal 59-type mono-vacancy appears in the curved area. Note that, the most stable mono-vacancy is the 5566 type that is located at the planar triangle area of Möbius strip. Our molecular dynamics simulations prove that both 5566- and 59-type mono-vacancy are stable at room

temperature. Furthermore, 5566-type mono-vacancy probably is a popular defects and can contribute  $sp^3$ -type spectral signals in the carbon based low-dimension materials with chiral twisting.

## ACKNOWLEDGEMENTS

This work was supported by the National Science Foundation of China under Grant No 11104276, 11174289 and 11174284, Knowledge Innovation Program of Chinese Academy of Sciences. Part of the calculations were performed in Center for Computational Science of CASHIPS.

- 
- [1] D. Ajami, O. Oeckler, A. Simon, and R. Herges, Nature (London) **426**, 819 (2003)
  - [2] R.P. John, M. Park, D. Moon, K. Lee, S. Hong, Y. Zou, C.S. Hong, and M.S. Lah, J. AM. Chem. Soc. **129**, 14142 (2007)
  - [3] J. Gravesen, M. Willatzen, Phys. Rev. A. **72**, 32108 (2005).
  - [4] N. Zhao, H. Dong, S. Yang, C.P. Sun, Phys. Rev. B. **79**, 125440 (2009).
  - [5] D.J. Ballon and H.U. Voss, Phys. Rev. Lett. **101**, 247701 (2008).
  - [6] D. Jiang and S. Dai, J. Phys. Chem. C. **112**, 5438 (2008).
  - [7] Z.L. Guo, Z.R. Gong, H. Dong and C.P. Sun, Phys. Rev. B. **80**, 195319 (2009).
  - [8] J.W. Jiang, J.S. Wang and B. Li, EPL. **89**, 46005 (2010).
  - [9] X.L. Wang, X.H. Zheng, M.Y. Ni, L. J. Zou, and Z. Zeng, Appl. Rev. Lett. **97**, 123103 (2010).
  - [10] Z. Li and L. R. Ram-Mohan, Phys. Rev. B. **85**, 195438 (2012).
  - [11] J. A. Nieto, R. Perez-Enriquez, arXiv preprint arXiv:1102.5748
  - [12] A. Hansson, M. Psulsson, and S. Stafström, Phys. Rev. B. **62**, 7639 (2000).
  - [13] P. Esquinazi, D. Spemann, R. Höhne, A. Setzer, K. -H. Han, and T. Butz, Phys. Rev. Lett. **91**, 227201 (2003).
  - [14] M. M. Ugeda, I. Brihuega, F. Guinea, and J. M. Gopez-Rodriguez, Phys. Rev. Lett. **104**, 096804 (2010).
  - [15] V. M. Pereira, F. Guinea, J. M. B. Lopes dos Santos, N. M. R. Peres, and A. H. Castro Neto, Phys. Rev. Lett. **96**, 036801 (2006).

- [16] L. Tapasztó, G. Dobrik, P. Nemes-Incze, G. Vertesy, Ph. Iambin, and L. P. Biró, Phys. Rev. B. **78**, 233407 (2008).
- [17] D. Teweldebrhan and A. A. Balandin, Appl. PHYS. Lett. **94**, 013101 (2009).
- [18] F. Banhart, J. Kotakoski, and A. V. Krasheninnikov, ACS. nano. **5**, 27 (2011).
- [19] A. Hashimoto, K. Suenaga, A. Gloter, K. Urita, and S. Iijima, Nature **430**, 870 (2004).
- [20] J. Kotakoski, A. V. Krasheninnikov, U. Kaiser, and J. C. Meyer, Phys. Rev. Lett. **106**, 105505 (2011).
- [21] K. Kim, H. J. Park, B. C. Woo, K. J. Kim, G. T. Kim, and W. S. Yun, Nano. Lett. **8**, 3092 (2008).
- [22] A.A. El-Barbary, R. H. Telling, C. P. Ewels, M. I. Heggie, and P. R. Briddon, Phys. Rev. B. **68**, 144107 (2003).
- [23] Y. Ma, P.O. Lehtinen, A. S. Foster, and R. M. Nieminen, New J. Phys. **6**, 68 (2004).
- [24] B. V. C. Martins and D. S. Galvão, Nano. Tech. **21**, 075710(2010).
- [25] V. B. Shenoy, C. D. Reddy, A. Ramasubramaniam, and Y. W. Zhang, Phys. Rev. Lett. **101**, 245501 (2008).
- [26] K. V. Bets and B. I. Yakobson, Nano. Res. **2**, 161 (2009).
- [27] H. Wang and M. Upmanyu, Phys. Rev. B. **86**, 205411 (2012).
- [28] Ying Li, J. Phys. D: Appl. Phys **43**, 495405 (2010).
- [29] X. L. Li, X. R. Wan, L. Zhang, S. Lee, and H. J. Dai, science **319**, 1229 (2008).
- [30] T. W. Chamberlain, J. Biskupek, G. A. Rance, A. Chuvilin, T. J. Alexander, E. Bichoutskaia, U. Kaiser, and A. N. Khlobystov, ACS nano **6**, 3943 (2012).
- [31] O. O. Kit, T. Tallinen, L. Mahadevan, J. Timonen, and P. Koskinen, Phys. Rev. B. **85**, 085428 (2012).
- [32] J.M. Soler, E. Artacho, J. D. Gale, A. García, J. Junquera, P. Ordejón, and D. Sánchez-Portal, J. Phys: Condens. Matter. **79**, 24745 (2002).
- [33] P. Ordejón, Phys. Status. Solidi. B. **217**, 335 (2000).
- [34] J. P. Perdew, K. Burke, and M. Ernzerhof, Phys. Rev. Lett **77**, 3865 (1996).
- [35] X. H. Zheng, X. L. Wang, L. F. Huang, H. Hao, J. Lan, and Z. Zeng, Phys. Rev. B. **86**, 081408 (2012).

TABLE I: Formation energies of mono-vacancy.

eV	graphene	MV-A	MV-B	MV-C
Formation energy	7.56	6.43	6.51	6.72



TABLE II: The structural properties of MV-A and MV-C. Distance ( $d$ ) and angle ( $a$ ) are shown in the unite of Å and degree, respectively.

	$d_{0-1}$	$d_{0-2}$	$d_{0-3}$	$d_{0-4}$	$a_{1-0-3}$	$a_{2-0-4}$	$a_{1-0-2}$	$a_{1-0-4}$
MV-A	1.62	1.67	1.60	1.68	138.0	147.6	96.2	96.1
MV-B	1.61	1.69	1.60	1.68	138.1	145.7	96.3	96.1

Fig. 1 Wang.eps

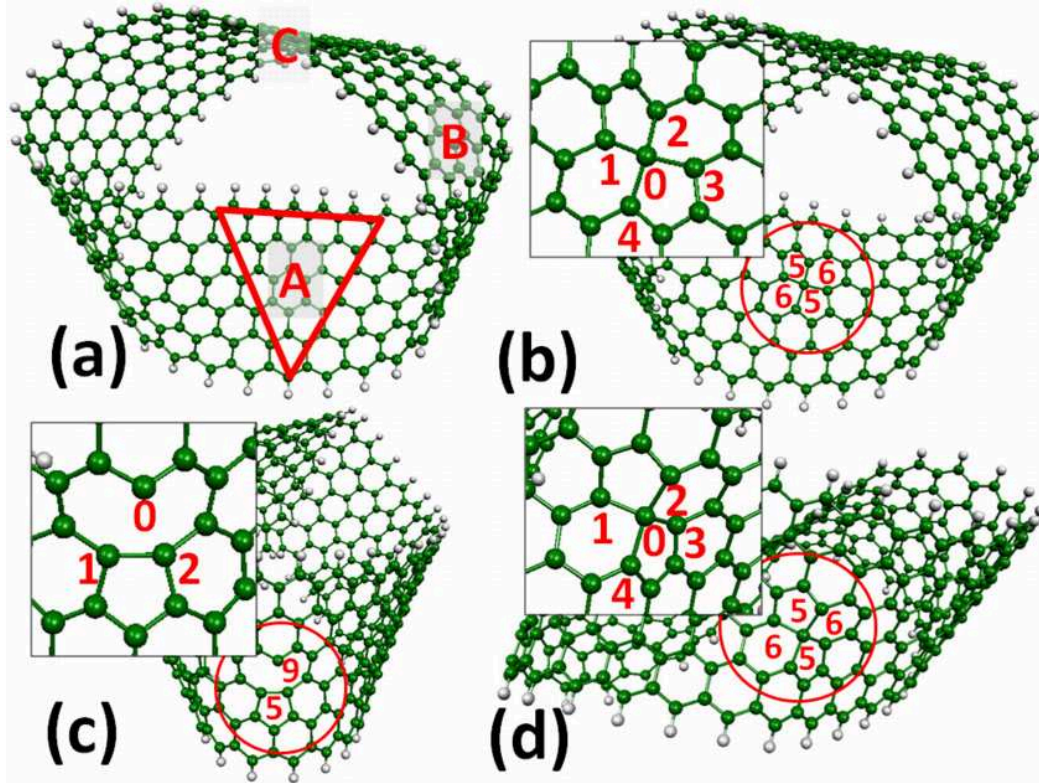


FIG. 1: (Color online)(a) The structure of ideal Möbius strip, and A, B and C are used to present the special areas to create MV. Red triangle shows the planar area. (b), (c) and (d) show the relaxed structures of MV introduced in the A(MV-A), B(MV-B) and C(MV-C) areas, respectively, while the enlarged structures are presented in the insets. The Arabic numbers presented in figures and insets are used to indicate the configurations and the atomic sites of MV, respectively.

Fig. 2 Wang.eps

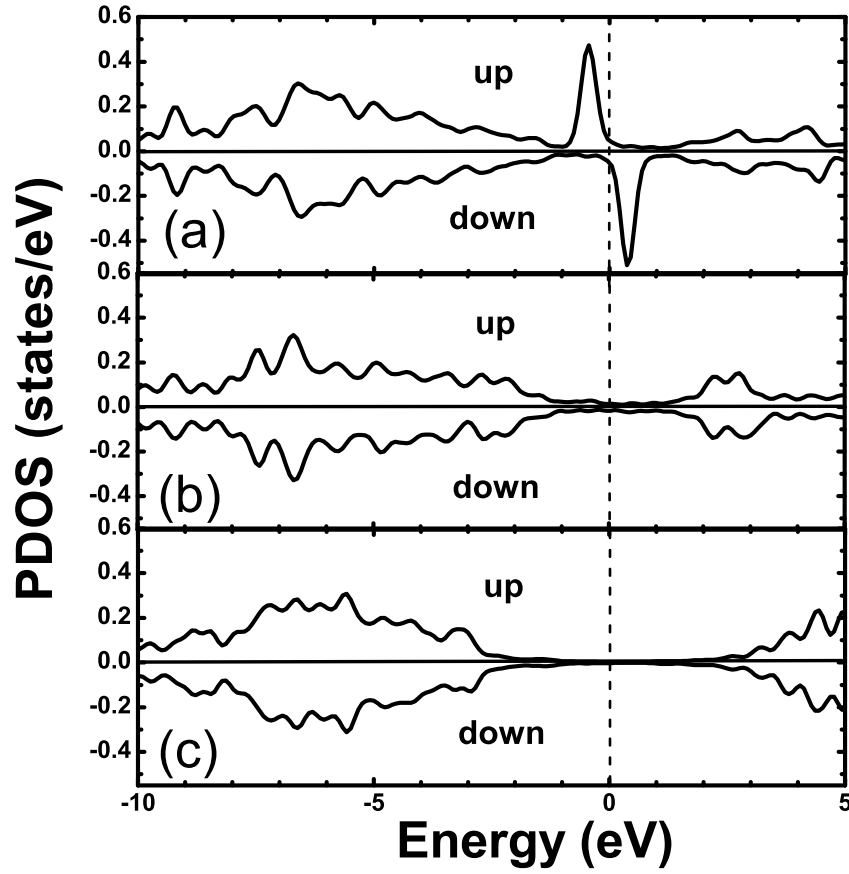


FIG. 2: The partial density of states (PDOS) of carbon atom located at the edge site of ideal Möbius strip (a), the central site of planar triangle area of ideal Möbius strip (b) and the central site of MV-A (c).

Fig. 3 Wang.eps

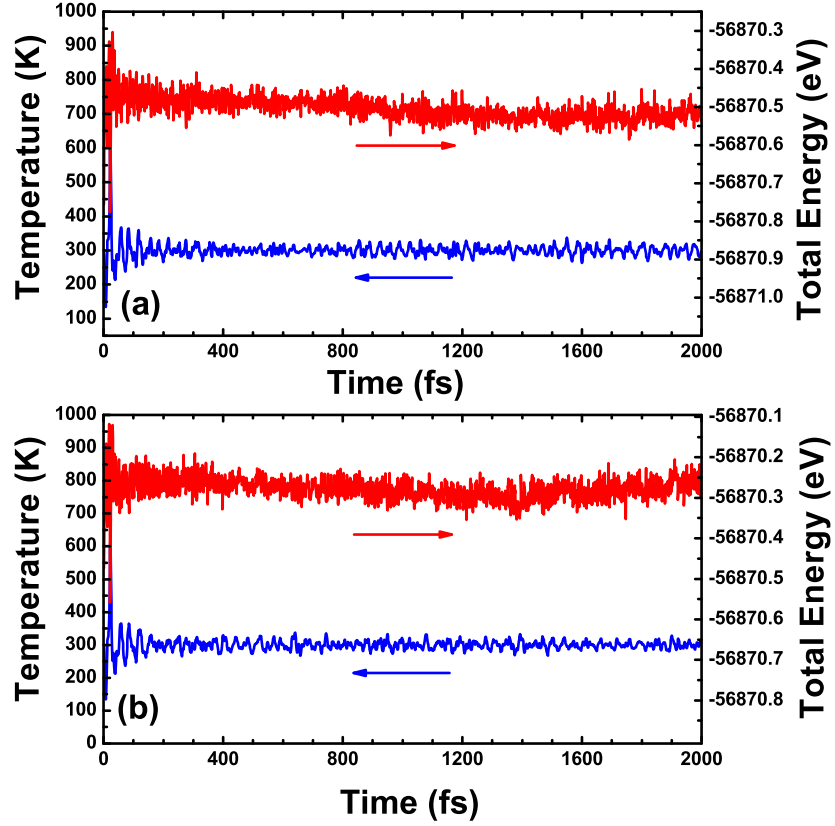


FIG. 3: (Color online) Changes of temperature and total energy as a function of time obtained from molecular dynamics simulations: (a) for MV-A, and (b) for MV-B.